Odd-mass nickel isotopes in a generalized-seniority approach

O. Monnoye,[1] S. Pittel,[2] J. Engel,[3] J. R. Bennett,[2,3,4] and P. Van Isacker[1]
[1]*Grand Accélérateur National d'Ions Lourds, BP 55027, F-14076 Caen Cedex 5, France*
[2]*Bartol Research Institute, University of Delaware, Newark, Delaware 19716*
[3]*Department of Physics and Astronomy, CB3255, University of North Carolina, Chapel Hill, North Carolina 27599-3255*
[4]*North Carolina School of Science and Mathematics, P.O. Box 2418, 1219 Broad Street, Durham, North Carolina 27715*
(Received 4 January 2002; published 1 April 2002)

The nickel isotopes exist over a wide range of neutron numbers, extending from proton-rich to very neutron-rich nuclei. Here we report a consistent study of the odd-mass $Z=28$ nuclei in the full $pf+g_{9/2}$ shell using the generalized-seniority shell model. We include up to three unpaired nucleons in the odd sector, and up to two in the even sector. We also report related results for the odd-mass ^{69}Cu and odd-odd ^{66}Co nuclei. Our calculations make use of a realistic shell-model interaction, whose monopole part has been renormalized to fit the properties of nuclei near closed shells. The calculated results are in good global agreement with experimental data, and contain some evidence of the persistence of the $N=40$ subshell closure around ^{68}Ni. The results demonstrate the importance of keeping the entire $pf+g_{9/2}$ space as active, both for neutrons and protons.

DOI: 10.1103/PhysRevC.65.044322 PACS number(s): 21.60.Cs, 21.60.Fw, 21.60.Ev

I. INTRODUCTION

The shell model [1] has been used for many years to describe the structure of nuclei, especially those that are fairly light or moderately near closed shells. With the steady improvement of computers, the size of the model spaces that can be accommodated has grown, expanding the region of nuclei that can be treated. For example, Caurier *et al.* [2] recently presented the results of a state-of-the-art shell-model study of even-even nuclei in the pf shell. Within that valence space, systems with dimensions of up to 10 000 000 were considered. Even so, some nuclear properties are not well explained with a valence space comprising a single major shell, suggesting the need for still larger model spaces. It is clear, however, that when the size of the single-particle valence space is increased, some truncation of the configuration space is necessary if calculations are to be carried out. One possibility is to use Monte Carlo methods [3,4]. Here we consider the application of an alternative truncation scheme, based on the use of the generalized-seniority [5] or broken-pair [6] approximation. This method has been widely used to approximate the shell model [7], especially when dealing with semimagic nuclei. Generalized seniority is approximately conserved by realistic Hamiltonians that involve only one type of nucleon. Most applications of the generalized-seniority truncation scheme have focussed on even-even semimagic nuclei, an example being a recent study of the tin isotopes with neutrons in the 50–82 shell [8]. Very little work has been done on odd-mass nuclei, where shell-model methods are invariably more difficult to implement. As we will see, the generalized seniority approximation to the shell model can be applied to odd-mass nuclei as well as even-even nuclei.

Recent experimental results on some neutron-rich nickel isotopes [9] exhibit features that remain unexplained in a shell-model study with a pf or a $pf_{5/2}g_{9/2}$ valence space. Because of the presumed semimagic character of these nuclides, a generalized-seniority truncation strategy should be appropriate for their description. We adopt such a strategy in the calculations reported here, using the full $pf+g_{9/2}$ valence space. We study the energy spectra, g factors, and β-decay properties of the odd-mass nickel isotopes between ^{57}Ni and ^{69}Ni. We also consider some isomeric states near the presumed $N=40$ subshell closure, for which magnetic dipole moments were measured recently [9].

The paper is organized as follows: After a brief description in Sec. II of the generalized-seniority scheme and its present implementation, in Sec. III we discuss our choice of an effective shell-model Hamiltonian for the $pf+g_{9/2}$ valence space. Section IV discusses the isospin-symmetry violation and spurious center-of-mass effects that arise in our calculations. In Sec. V, results for various calculated observables (energy spectra, g factors, β decay) are presented for the nickel isotopes and also for a few nuclei close to ^{68}Ni for which data have recently become available. Finally, in Sec. VI, we summarize our results and make some global statements about the persistence of the $N=40$ subshell closure around ^{68}Ni.

II. GENERALIZED-SENIORITY APPROXIMATION

A brief overview is presented here of the techniques used to truncate the shell-model basis in a generalized-seniority approach. For more details, the reader is referred to, for example, the review article by Allaart *et al.* [7] or the paper by Pittel *et al.* [10].

The generalized-seniority scheme is based on the idea that there exists some energetically favored (correlated) pair, called the S pair, of identical valence nucleons coupled to angular momentum zero. In the generalized-seniority approximation, the ground state of an even-even semimagic nucleus is a condensate of $n/2$ S pairs, where n is the number of valence nucleons. In the same approximation, the low-lying states are described in terms of states with progressively fewer S pairs. The generalized-seniority quantum number v is defined as the number of valence nucleons that are not in S pairs. Hence the low-energy states of (semimagic) nuclei are states of low generalized seniority.

The first step toward a generalized-seniority description of a given nucleus consists of finding the structure of the collective S pair. In second quantization, it is defined as

$$S^\dagger = \sum_{i=1}^{m} \alpha_i \frac{1}{2}\sqrt{2j_i+1}[a_i^\dagger a_i^\dagger]_0^{(0)}, \tag{1}$$

where the sum runs over the m single-particle orbits of the valence space, j_i represents the angular momentum of orbit i, and α_i is related to its occupancy. In the simplest generalized-seniority approximation, the ground state of an even-even semimagic nucleus with n identical nucleons in the valence shell is assumed to have the form

$$(S^\dagger)^{n/2}|o\rangle, \tag{2}$$

where the doubly-magic core nucleus plays the role of the vacuum $|o\rangle$. In the case of n_ν active neutrons and n_π active protons, the state of lowest generalized seniority (of an even-even nucleus) is

$$(S_\nu^\dagger)^{n_\nu/2}(S_\pi^\dagger)^{n_\pi/2}|o\rangle. \tag{3}$$

Such a state is said to have a generalized seniority 0 for neutrons and a generalized seniority 0 for protons. Where not confusing, we will sometimes refer to a state in terms of its total generalized seniority, defined as the sum of the generalized seniorities carried by neutrons and protons.

In our calculations, we determine the structure coefficients α_i that define the collective S pairs through a minimization of the expectation value of the shell-model Hamiltonian (see Sec. III) in the normalized trial state [Eq. (3)]. This energy minimization is obtained with an iterative diagonalization procedure [11], as this has been shown to be numerically more stable than other optimization strategies. For an odd-mass or odd-odd nucleus, the α_i are taken from a close-by even-even nucleus.

Once the structure of the S pair has been determined for both neutrons and protons, the shell-model problem can be solved in a truncated space of low generalized seniority. Our computer implementation of this approach allows one broken S pair for both valence neutrons and protons. Thus, for an odd-mass nucleus, we allow states with up to five uncoupled nucleons, i.e., three neutrons and two protons, or vice versa. The dimension reduction implied by this truncation of the configuration space is illustrated with some examples in Table I.

With such a truncation, the size of the space does not grow as we proceed further from closed shells. On the other hand, nuclei with reasonably large numbers of valence neutrons and protons tend to exhibit strong quadrupole collectivity which mixes large numbers of generalized-seniority configurations, including those with generalized seniorities beyond the capabilities of our codes. Our study is therefore limited to nuclei that are either semimagic or nearly semimagic.

An aspect of our approach that should be emphasized is that the semimagic nature of the nucleus under study need *not* be explicitly imposed, but rather may arise as an outcome of the calculation. To illustrate this point, consider the nucleus ^{67}Ni, which we describe as eight protons and 19 neutrons outside a ^{40}Ca core moving in a $pf+g_{9/2}$ valence space. As such, $Z=28$ closure is not imposed explicitly. If it is found that this closure survives the shell-model interaction, then the generalized-seniority approximation can be trusted. On the other hand, a disappearance of the closure would drive the nucleus toward deformation (as a result of the interactions between the valence neutrons *and* protons), and would destroy the validity of the generalized-seniority approximation. Of course, it should be borne in mind that there may be some states in such a nucleus in which the $Z=28$ closure is approximately preserved and others in which it is not. Such coexistence phenomena near closed shells are well known, including in the region around ^{56}Ni. The semimagic nature of the $N=40$ isotones and the applicability of the generalized-seniority approximation in this regime can be discussed in similar terms.

TABLE I. Comparison between the dimensions of the full $pf+g_{9/2}$ shell-model basis and those of the generalized-seniority calculations carried out in this paper. In all cases the dimension shown is for the $\frac{1}{2}^-$ subspace.

Nucleus	Shell-model dimension	Generalized-seniority dimension	
		$v_n=1, v_p\leqslant 2$	$v\leqslant 3, v_p\leqslant 2$
^{41}Ca	1	1	1
^{77}Ni	153 490	54	54
^{75}Ni	15 132 228	54	2 961
^{73}Ni	423 564 622	54	2 961
^{67}Ni	113 433 116 020	54	2 961
^{57}Ni	32 126 859 970	54	2 961

To test our code implementation, we have considered some analytically solvable shell-model problems; these include the SU(3) rotational model of Elliott [12] and the SO(8) pairing model of Flowers and Szpikowski [13]. The analytical and numerical results are in exact agreement when we are sufficiently near shell closures so that no truncation of the shell-model basis is made. This indicates that our code works correctly.

In the next sections, we describe the generalized-seniority shell-model calculations that we carried out for the nickel isotopes and for several other nuclides in the vicinity of $N=40$. We begin with a discussion of the effective shell-model Hamiltonian used in the $pf+g_{9/2}$ valence space.

III. SHELL-MODEL INTERACTION

Our aim here is to calculate the properties of the *entire* chain of nickel isotopes, from the proton-rich side of the valley of stability to its neutron-rich side up to and including $N=40$, using a single model space and a single effective Hamiltonian. As noted earlier, the model space we use involves the full $pf+g_{9/2}$ shell. In defining the effective Hamiltonian for this enlarged model space, we would like, on the one hand, that it be as realistic as possible and, on the other hand, that it be tailored to reproduce the global trends

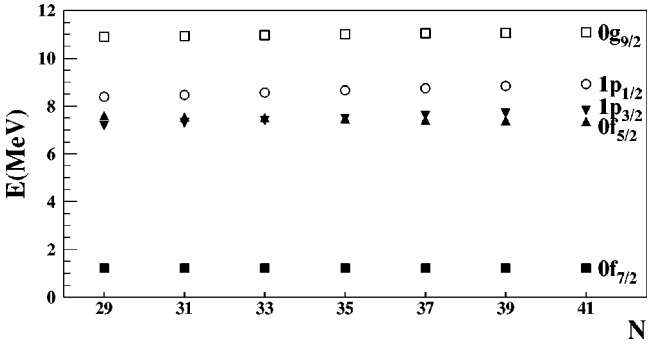

FIG. 1. Effective single-particle energies as a function of neutron number as deduced from the renormalized monopole part of the shell-model interaction.

of the energy spectra of nuclei from one end to the other of the $20 \leqslant N,Z \leqslant 50$ shell.

With this in mind, we proceed as follows. We start with an effective *G*-matrix [14] interaction derived for the $pf+g_{9/2}$ valence space [15]. We then correct its monopole part following the prescription of Zuker *et al.* [16]. The various monopoles are finetuned using the known low-lying levels in ^{57}Ni and ^{89}Zr, while the single-particle energies are taken from the experimental ^{41}Ca spectrum for the $0f_{7/2}$, $0f_{5/2}$, $1p_{1/2}$, and $1p_{3/2}$ orbits, and from Ref. [17] for the $0g_{9/2}$. The resulting parametrization of the monopole part assumes a smooth linear evolution of the effective single-particle energies with valence particle number, as shown in Fig. 1. We note at this point that the $0f_{7/2}$ single-particle level may be a little too low, leading to a ^{56}Ni ''core'' that is too stiff (i.e., not easily excitable).

IV. ISOSPIN SYMMETRY BREAKING AND SPURIOUS CENTER-OF-MASS MOTION

Both our choice of a generalized-seniority truncation scheme and our assumption of a $pf+g_{9/2}$ valence space introduce some nonphysical effects in calculated observables. The generalized-seniority scheme is based on a *weak coupling* of neutron states to proton states. Unless all states in the two spaces are maintained—which is not the case in the presence of a generalized-seniority truncation—some violation of the isospin symmetry will creep into the wave functions that result, even if the underlying Hamiltonian is an isospin scalar. Spurious admixtures of components in which the center of mass has been excited will likewise show up in the wave functions of such a theory, when the valence space does not involve complete harmonic-oscillator shells. The proper elimination of these spurious effects is very difficult and we do not attempt it here. Nevertheless, an unambiguous method exists to calculate the admixtures of spurious center-of-mass components or the amount of isospin mixing in a given eigenfunction. They can be derived from the expectation values

$$\langle \Psi|\hat{T}^2|\Psi\rangle \text{ and } \langle \Psi|\hat{O}_A|\Psi\rangle \equiv \langle \Psi|\frac{\hat{P}^2}{2mA}+\frac{1}{2}m\omega^2 A\hat{R}^2|\Psi\rangle, \tag{4}$$

TABLE II. Lower bounds for c_T^2 and c_0^2—as defined in the text—which give the degree of isospin impurity and spurious center-of-mass admixtures, respectively, in the ground states of the nickel isotopes.

Nucleus	^{57}Ni	^{59}Ni	^{61}Ni	^{63}Ni	^{65}Ni	^{67}Ni	^{69}Ni
$c_T^2 \geqslant$	0.976	0.988	0.992	0.994	0.995	0.997	0.998
$c_0^2 \geqslant$	0.990	0.995	0.995	0.994	0.994	0.993	0.993

where $\hat{T}_\mu \equiv \Sigma_i t_\mu(i)$ are the components of the isospin vector while $\hat{R}_\mu \equiv (1/A)\Sigma_i r_\mu(i)$ and $\hat{P}_\mu \equiv \Sigma_i p_\mu(i)$ are the center-of-mass coordinate and the total momentum of the nucleus.

While the eigenstates $|\Psi\rangle$ obtained from a truncated shell-model calculation do not in general carry good isospin *T*, they can always be expanded in an isospin basis

$$|\Psi\rangle = c_T|\Psi_T\rangle + c_{T+1}|\Psi_{T+1}\rangle + \cdots, \tag{5}$$

where T is the lowest possible isospin, viz $T=|T_z| = \frac{1}{2}|N-Z|$. In all cases (with the exception of some odd-odd $N=Z$ nuclei) the low-energy states have $T=|T_z|$ and an untruncated calculation with an isospin-invariant shell-model interaction yields $c_T=1$ with all other coefficients zero. Thus, in a truncated calculation, the extent to which c_T is smaller than 1 indicates the degree of isospin mixing in the state. It is a matter of simple algebra to find the following lower bound for c_T:

$$c_T^2 \geqslant \frac{(T+1)(T+2)-\langle \Psi|\hat{T}^2|\Psi\rangle}{2(T+1)}. \tag{6}$$

Likewise, the coefficient c_0 in the expansion

$$|\Psi\rangle = c_0|\Psi_{N=0}\rangle + c_1|\Psi_{N=1}\rangle + \cdots, \tag{7}$$

where N is the number of quanta in the spurious center-of-mass motion, can be given the following lower bound:

$$c_0^2 \geqslant \frac{5}{2} - \frac{\langle \Psi|\hat{O}_A|\Psi\rangle}{\hbar\omega}. \tag{8}$$

These bounds enable us to measure the extent to which a given state preserves the relevant symmetries of the system, and thus to establish a criterion for deciding which states to leave out from further investigation and interpretation. Table II shows the lower limits [Eqs. (6) and (8)] in the ground states of the nickel isotopes calculated in this work. The spurious center-of-mass components and the higher-isospin admixtures are in all cases quite small, suggesting that neither the generalized-seniority truncation nor the assumed valence space produce large unphysical components in these states. Note that the admixture of higher-isospin components, as expected, decreases as the neutron excess grows. Furthermore, even in the nuclei with $N \approx Z$, where the effect is largest, the violation of isospin symmetry induced by the truncation is small. The admixture of spurious center-of-mass

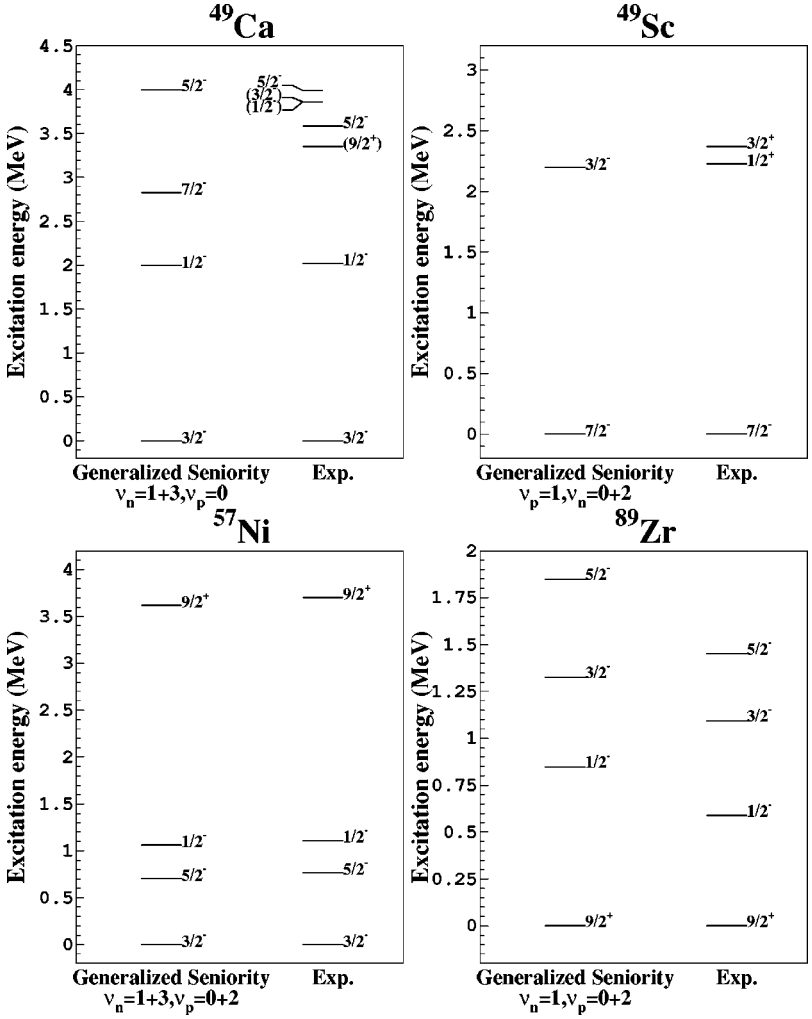

FIG. 2. Energy spectra of the nuclei used to fine tune the monopole part of the shell-model interaction.

components does not vary substantially with neutron number, as it reflects the valence space itself rather than the truncation scheme.

Any state shown in the spectra of Sec. V has been tested according to the above criteria. If it contains no significant component with spurious center-of-mass motion it is kept for further study. As isospin mixing may play a role in β-decay studies, even for small admixtures, we discuss this issue further in the next section.

V. RESULTS

A logical way to proceed with the calculations is to first perform them for nuclei close to the valley of stability, where a large body of data is available, and then to extend them to those isotopes on the neutron-rich side that have been the subject of recent experimental study. Particular attention has been paid to the evolution of the energy spectra, ground-state g factors, and β-decay lifetimes as a function of neutron number. A final part of this section is devoted to the recently measured g factors of some isomeric states in the vicinity of ^{68}Ni (see Fig. 2).

A. Energy spectra

Figures 3 and 4 show a comparison between the calculated and observed nickel spectra. Agreement with experiment can be noted for the lowest levels. It is clear, however, that beyond a given excitation energy many more levels are observed than can be accounted for theoretically. A clear example of this is seen in the spectrum of ^{57}Ni. The low-energy states have a dominant generalized-seniority $v=1$ component and are correctly accounted for in the calculation. At energies of about 2.5 MeV and upward, many levels appear in the experimental spectrum with no theoretical counterparts. One possibility is that the experimental levels in that region are predominantly of generalized-seniority $v=3$ character. Theory indeed produces many $v=3$ states, but at much higher energies. Note that to produce a $v=3$ state, we must promote at least one particle across the $N=Z=28$ shell gap. As noted earlier, the $f_{7/2}$ level may be placed a bit too low by our single-particle Hamiltonian, leading to $v=3$ excitations too high in energy.

Another possibility is that some of the experimental states have a deformed character, built on the 4.5 MeV intruder band in ^{56}Ni [4]. Such states cannot be accommodated in a theory truncated to low generalized-seniority configurations only, but should go up in energy as we progressively add neutrons to ^{56}Ni.

According to Figs. 3 and 4, the theoretical $v=3$ levels come down in energy as a function of increasing neutron number. This reflects the fact that neutron excitations across

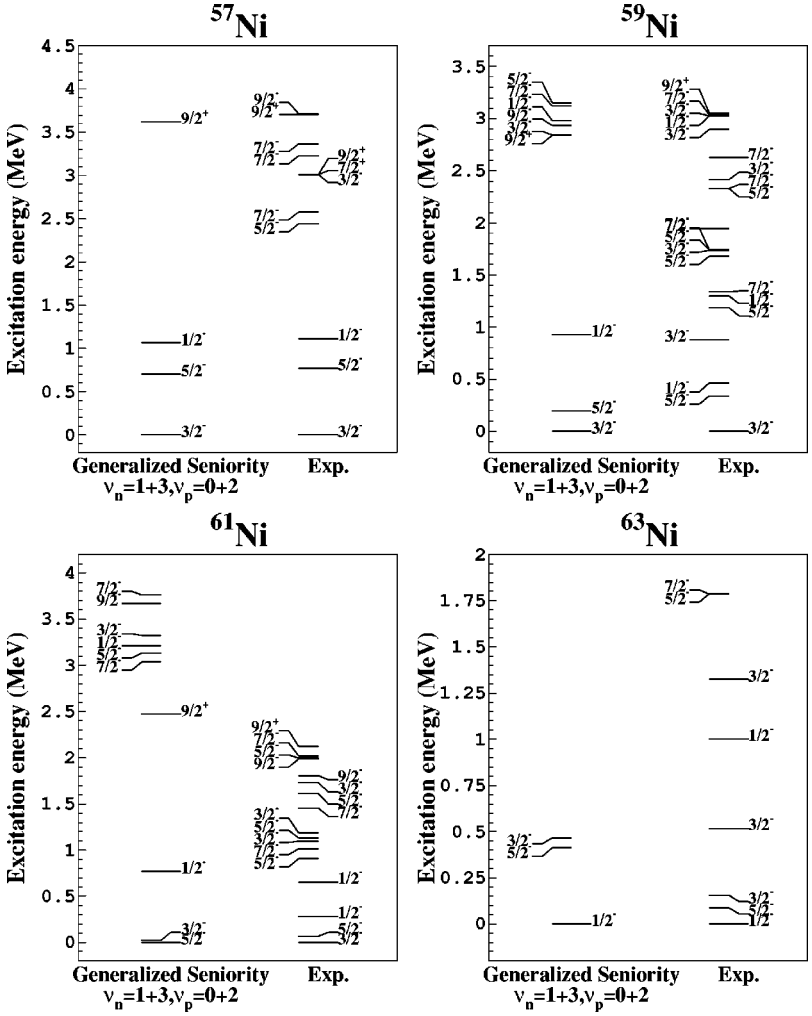

FIG. 3. Spectra of the odd-mass nickel isotopes from ^{57}Ni to ^{63}Ni. The experimental spectra are limited to the lowest-lying levels and are taken from Ref. [18] for ^{57}Ni and from Ref. [22] for the other nuclei.

the $N=28$ gap are no longer required to produce $v=3$ states. The experimental levels likewise come down in energy with the addition of neutrons. It is our belief that these are also $v=3$ states, as the intruder states have presumably left the energy window under discussion. With this interpretation, we conclude that the splitting between $v=1$ and 3 levels remains too large in our calculations throughout the entire series of nickel isotopes.

Our explanation of why the theoretical spectrum is much less compressed than the experimental spectrum focused on the single-particle gap at the 28 subshell closure being too large. As noted earlier, this arose by assuming a linear evolution of single-particle energies and fitting to the properties of single-particle or single-hole nuclei. Different parametrizations of the monopole interaction could conceivably change the magnitude of this gap in the vicinity of ^{56}Ni and improve the quality of the agreement. One possibility might be to consider a more complex parametrization that takes into account not only the valence particle number but also the occupation numbers of the various orbits.

B. *g* factors

The results in this subsection primarily concern g factors of the ground states of the nickel isotopes considered previously. This property is not known experimentally for all isotopes. In all cases, our results can be compared to the so-called Schmidt values, which correspond to the g factors obtained in the independent-particle model. All theoretical results are calculated with a spin-quenching factor of 0.7 to account for in-medium effects on the free neutron and proton spin g factors. The comparison between calculated and experimental results is shown in Fig. 5. The data are represented with open circles, while the Schmidt limits are drawn as dotted lines. Two levels of approximation are shown for the generalized-seniority calculations. The first allows only one neutron not in an S pair (i.e., generalized seniority $v_\nu=1$ for the neutrons), and is represented by open squares. The second allows up to a generalized seniority $v_\nu=3$ for the neutrons, and is shown by solid squares. In both cases, up to a generalized seniority $v_\pi=2$ is allowed for the protons. In the following, the first level of approximation is referred to as GS-1 and the second as GS-3.

The calculated results show general agreement with the data. Moreover, in most cases the agreement improves with the inclusion of correlations, i.e., going from the independent-particle result (Schmidt limit) to the GS-3 result. This is particularly true for the lighter isotopes, suggesting that our description of correlations in the ground states of

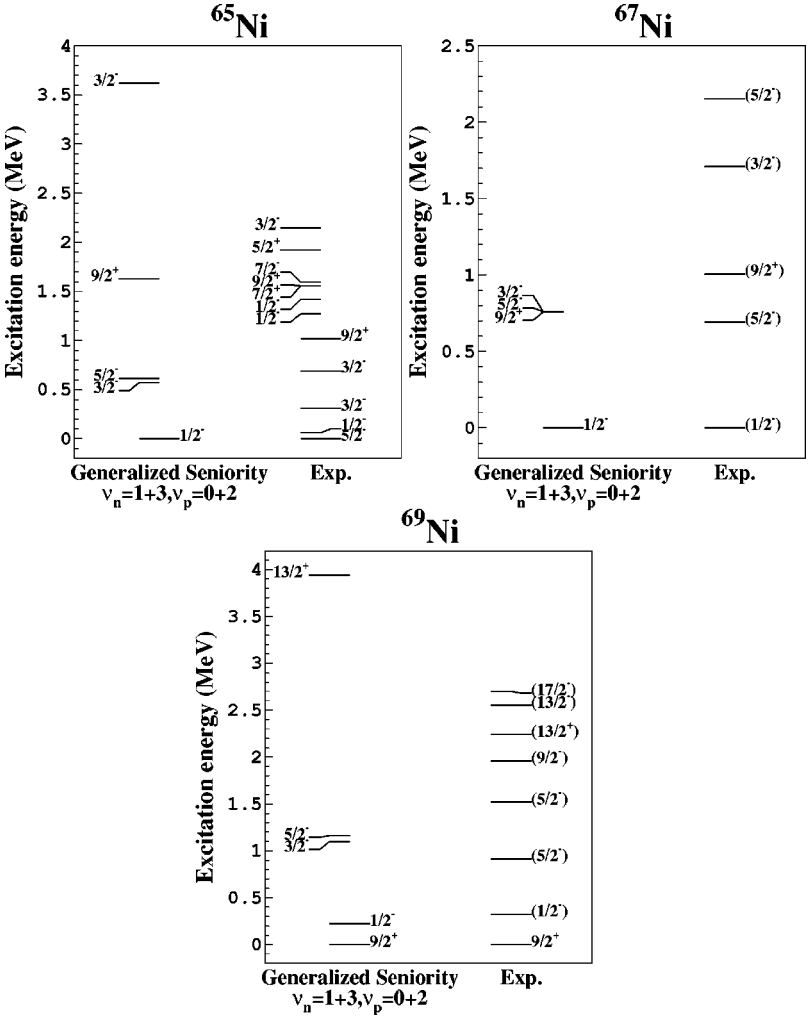

FIG. 4. Spectra of the odd-mass nickel isotopes from ^{65}Ni to ^{69}Ni. The experimental spectra are limited to the lowest-lying levels and are taken from Ref. [22] for ^{65}Ni, from Ref. [19,20] for ^{67}Ni, and from Ref. [21] for ^{69}Ni.

these nuclei is reasonable. The results for the heavier ^{63}Ni and ^{65}Ni isotopes are more difficult to interpret in light of the lack of experimental data. We simply note that the oscillation of the GS-1 and GS-3 results around the Schmidt values is most likely a reflection of the complex configuration mixing that occurs between the $p_{1/2}$ and $f_{5/2}$ orbits in this region. The case of ^{67}Ni is exceptional. The discrepancy between the calculated and experimental results actually grows as the level of generalized-seniority approximation increases, i.e., the discrepancy is larger for GS-3 than for GS-1. A possible explanation is that all g factors are calculated assuming a constant quenching for the spin matrix elements. A recent paper [26] showed that this need not always be the case and, in particular, that in ^{67}Ni free-nucleon g factors should be taken. The result for ^{67}Ni obtained without a spin quenching factor is represented in the figure by a triangle. Note that it is in much better agreement with experiment.

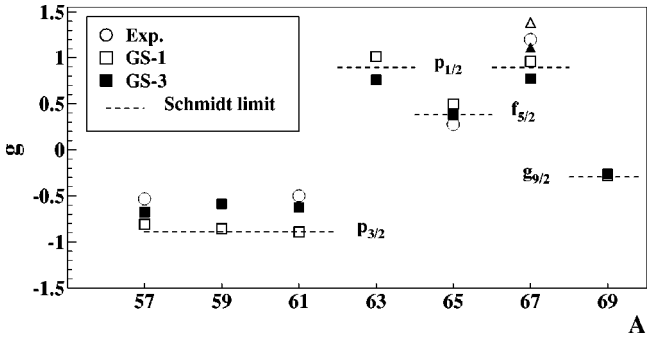

FIG. 5. Comparison between calculated results and measured g factors for the ground states of the odd-mass nickel isotopes as a function of the mass number A. The experimental results are taken from Refs. [23–26]. For an explanation of the symbols used in the figure, see the text.

To give some idea of the variation with mass of the calculated magnetic moments of specific states, these are shown in Table III for yrast states with $J^\pi = \frac{1}{2}^-$, $\frac{3}{2}^-$, $\frac{5}{2}^-$, and $\frac{9}{2}^+$. The results are obtained in the GS-3 approximation with free neutron and proton g factors. The main conclusion is that only very smooth variations with particle number occur.

C. β-decay lifetimes

Another observable that is very sensitive to the structure of nuclei is the Gamow-Teller β^--decay rate. Figure 6 shows results for the Gamow-Teller decays from the odd-mass nickel isotopes to the relevant odd-mass daughter states in copper. The figure includes a comparison between the measured lifetimes, the GS-1 and GS-3 results, and those of the

TABLE III. Calculated magnetic moments of some yrast states in the odd-mass nickel isotopes.

Nucleus	$\mu(\frac{1}{2}^-)$	$\mu(\frac{3}{2}^-)$	$\mu(\frac{5}{2}^-)$	$\mu(\frac{9}{2}^+)$
^{57}Ni	0.41	−1.01	0.97	−1.03
^{59}Ni	0.37	−0.94	0.91	−1.07
^{61}Ni	0.37	−0.93	0.88	−1.06
^{63}Ni	0.38	−0.93	0.94	−1.08
^{65}Ni	0.39	−0.97	0.95	−1.11
^{67}Ni	0.39	−0.98	1.02	−1.13
^{69}Ni	0.36	−0.94	0.96	−1.17

finite-range droplet model of Möller *et al.* [27]. The GS-1 results are represented by open squares and the GS-3 results by full squares. Experimental values are shown as open squares. Möller *et al.*'s tables give definite values only for lifetimes shorter than 100 s. For longer lifetimes only the bound is indicated. These results are shown as full circles, with upward arrows in those cases that have no definite value. Since the renormalization of the monopole interaction has been determined from excitation energies only and not from binding energies, we cannot expect the shell-model calculation to reproduce the correct binding energies of the parent and daughter nuclei. We therefore use the *experimental* β-decay Q values in our lifetime calculations. The calculated results are in global agreement with the data, particularly when approaching the $N=40$ subshell closure. This may be related to the smallness of the isospin admixtures in these neutron-rich nuclides (see Table II). Even in the lighter isotopes ^{63}Ni and ^{65}Ni, where we underestimate the lifetimes by more than an order of magnitude, our approach gives better results than those of Möller *et al.* In all nuclei except ^{65}Ni, the lifetimes calculated with GS-1 and GS-3 are very similar (in fact the latter are a little shorter). This is because the generalized-seniority $v=3$ states lie above the narrow Q-value window. In ^{65}Ni however, one state of mainly generalized-seniority $v=3$ character lies in the Q-value window, resulting in a dramatic change in the lifetime.

D. $N=40$ subshell closure

Experimental studies have been carried out recently at GANIL in the vicinity of ^{68}Ni [9] to test the closed character

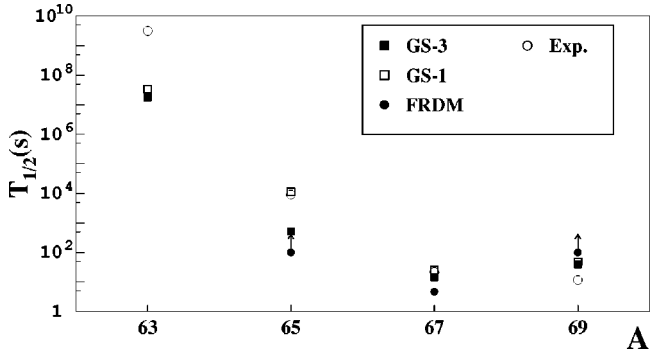

FIG. 6. Measured and calculated β-decay lifetimes for the odd-mass nickel isotopes as a function of the mass number A. For an explanation of the symbols used in the figure, see the text.

of the $N=40$ subshell. The g factors of μs isomers of nickel, copper, and cobalt isotopes with $N=40$ have been measured since they provide valuable information relevant to this question. The model space used in our work is ideally suited for a theoretical investigation of these isomers, as it does not limit the excitation of neutrons any more than that of protons. We first report results on the energy spectra of the different nuclei, and then turn to the g factors of the corresponding isomers.

1. Spectra

Figure 7 shows a comparison between the calculated and experimental spectra of the nuclei under investigation, namely, ^{67}Ni, ^{69}Cu, and ^{66}Co. These three nuclei bear directly on the question of the $N=40$ and $Z=28$ (sub)shell closures away from the valley of stability: all have either $N=40$ or $Z=28$ or lie within one nucleon of these magic numbers.

The odd-mass nuclei, ^{67}Ni and ^{69}Cu, are reasonably well reproduced by the calculation. The ground-state spins and parities are correctly given and excited states with the correct spin and parity are found among those at low excitation energy. Experiment shows many levels between 1 and 3 MeV in ^{69}Cu that are not produced by the calculation. There are several possible reasons for this disagreement. On the one hand, the fact that the effective shell gap at the 28 closed shell is too large could still have an effect on the location of states with $v=3$ and, even more so, $v=5$, producing such states too high in excitation energy, analogous to its effect in the nickel isotopes. At the same time, states with even higher generalized seniorities, outside the scope of our calculations, could also be playing some role. Not much is known experimentally in ^{66}Co: the ground state probably has 3^+; the exact excitation energy of the isomer is unknown. Two possible configurations $\overline{\pi}_{f_{7/2}}\otimes\overline{\nu}_{p_{1/2}}$ or $\overline{\pi}_{f_{7/2}}\otimes\nu_{g_{9/2}}$ lead to a likely 4^+ or 7^- assignment.

2. g factors

Table IV shows the calculated and recently measured g factors of the isomeric states in ^{67}Ni, ^{69}Cu, and ^{66}Co. The spin and parity of the isomer is also specified as is its dominant single-particle configuration. The generalized-seniority results are close to the Schmidt values for ^{67}Ni and ^{66}Co, but fairly far from the experimental values. In ^{69}Cu, there is a strong modification to the Schmidt value seen experimentally, and it is well reproduced by the GS-3 calculation. This is a consequence of a fairly strong mixing between the dominant configuration and others (most notably a configuration with $\pi_{p_{3/2}}\otimes\overline{\nu}_{f_{5/2}}\nu_{g_{9/2}}$).

In the case of ^{67}Ni it seems that the generalized-seniority approach or, alternatively, the shell-model interaction, does not induce enough mixing to describe the experimental situation. On the other hand, the GS-3 calculation gives a second $\frac{9}{2}^+$ level with a g factor of -0.182. This state has a large component with $\overline{\pi}_{f_{7/2}}\pi_{p_{3/2}}\otimes\nu_{g_{9/2}}$ character, for which the single-particle g factor is -0.123. This second $\frac{9}{2}^+$ level, however, is produced more than 4 MeV too high in energy

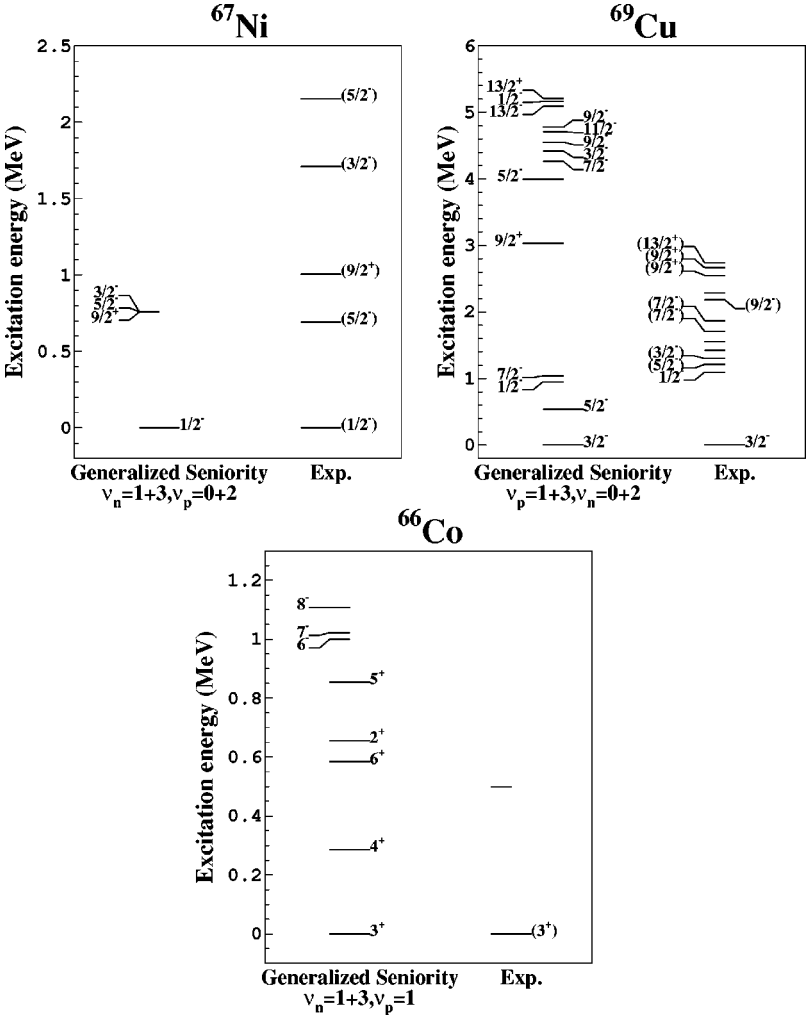

FIG. 7. Calculated and observed spectra (as taken from Refs. [19,20,22,28]) for the $N \simeq 40$ and $Z \simeq 28$ nuclei under investigation. The excitation energy of the isomeric level in ^{66}Co is not known experimentally, and is arbitrarily put at 500 keV.

by the calculation. It could be brought down by a decrease in the shell gap at $Z=28$, through a modification of the monopole interaction involving the $f_{7/2}$ orbit. This would also presumably change the g factor and, as noted earlier, the spectrum of ^{66}Co.

VI. CONCLUSIONS

The approximate semimagic nature of the nickel isotopes has made it possible for us to meaningfully treat them within the generalized-seniority shell model. In order to shed light on the evolution of the $N=40$ subshell closure, we have used this truncation method to systematically determine the structure of the odd-mass nickel isotopes from ^{57}Ni to ^{69}Ni and to investigate some other nuclei that are close to ^{68}Ni. The $pf+g_{9/2}$ model space that we used allows excitations across the 28-shell gap for both neutrons and protons, and this made it possible to address issues related to the $N=40$ and $Z=28$ (sub)shell closures. The interaction that we used with this model space contained a renormalized monopole part, obtained by a fit to the spectra of ^{41}Ca, ^{57}Ni, and ^{89}Zr. The resulting calculated spectra and g factors showed fairly good global agreement with the experimental observables, and indicated the persistence of the $N=40$ subshell closure. However, our results lack in precision for the neutron-rich $N \simeq 40$ isotopes, as a comparison with recently measured g

TABLE IV. Comparison between calculated and measured g factors for isomeric states in ^{67}Ni, ^{69}Cu, and ^{66}Co. The experimental values are taken from Ref. [9].

Nucleus	^{67}Ni	^{69}Cu	^{66}Co		
Isomer's J^π	$\frac{9}{2}^+$	$\frac{13}{2}^+$	4^+	or	7^-
S.p. configuration	$\nu_{g_{9/2}}$	$\pi_{p_{3/2}} \otimes \overline{\nu}_{p_{1/2}} \nu_{g_{9/2}}$	$\overline{\pi}_{f_{7/2}} \otimes \overline{\nu}_{p_{1/2}}$	or	$\overline{\pi}_{f_{7/2}} \otimes \nu_{g_{9/2}}$
S.p. g factor	-0.297	0.375	1.350	or	0.421
GS-3 g factor	-0.252	0.241	1.311	or	0.402
Measured g factor	$-0.1245(60)$	0.219(33)		0.157(9)	

factors showed. We believe that this limitation is most likely related to the monopole part of the interaction, and does not affect our conclusions on the need for the expanded model space that we have used (as can be seen in some excited states of $Z \simeq 28, N \simeq 40$ nuclei). We thus suggest that further studies be made within this model space, but with a more sophisticated interaction.

ACKNOWLEDGMENTS

This work was supported in part by the National Science Foundation under Grant Nos. PHY-9600445, PHY-9970749, and INT-9415876, in part by the Department of Energy under Grant No. DE-FG02-97ER41019, and in part by the Centre National de Recherche Scientifique (France).

[1] M.G. Mayer, Phys. Rev. **75**, 1969 (1949).
[2] E. Caurier *et al.*, Nucl. Phys. **A653**, 439 (1999).
[3] D. Dean, S. Koonin, K. Langanke, and P. Radha, Phys. Lett. B **399**, 1 (1997).
[4] T. Otsuka, T. Mizusaki, and M. Honma, J. Phys. G **25**, 699 (1999).
[5] I. Talmi, Nucl. Phys. **A172**, 1 (1971).
[6] Y.K. Gambhir, A. Rimini, and T. Weber, Phys. Rev. **188**, 1573 (1969).
[7] K. Allaart *et al.*, Phys. Rep. **169**, 209 (1988).
[8] N. Sandulescu *et al.*, Phys. Rev. C **55**, 2708 (1997).
[9] G. Georgiev, Ph.D. thesis, Katholieke Universiteit Leuven, 2001.
[10] S. Pittel, P.D. Duval, and B.R. Barrett, Ann. Phys. (N.Y.) **144**, 168 (1982).
[11] O. Scholten, Phys. Rev. C **28**, 1783 (1983).
[12] J.P. Elliott, Proc. R. Soc. London, Ser. A **245**, 128 (1958).
[13] B.H. Flowers and S. Szpikowski, Proc. Phys. Soc. London **84**, 673 (1964).
[14] K.A. Brueckner, Phys. Rev. **97**, 1353 (1955).
[15] M. Hjorth-Jensen *et al.*, Phys. Rep. **261**, 125 (1995).
[16] A.P. Zuker and M. Dufour, nucl-th/9505012.
[17] J. Duflo and A.P. Zuker, Phys. Rev. C **59**, R2347 (1999).
[18] D. Rudolph *et al.*, Eur. Phys. J. A **6**, 377 (1999).
[19] L. Weissman *et al.*, Phys. Rev. C **59**, 2004 (1999).
[20] M. Girod *et al.*, Phys. Rev. C **37**, 2600 (1988).
[21] R. Grzywacz *et al.*, Phys. Rev. Lett. **81**, 766 (1998).
[22] R.B. Firestone, *Table of Isotopes* (Wiley Interscience, New York, 1996).
[23] M.R. Bhat, Nucl. Data Sheets **69**, 209 (1993).
[24] M.R. Bhat, Nucl. Data Sheets **85**, 415 (1998).
[25] M.R. Bhat, Nucl. Data Sheets **88**, 417 (1999).
[26] J. Rikovska *et al.*, Phys. Rev. Lett. **85**, 1392 (2000).
[27] P. Möller, J.R. Nix, and K.-L. Kratz, Acta Math. **66**, 131 (1997).
[28] A.M. Oros-Peusquens and P.F. Mantica, Nucl. Phys. **A669**, 81 (2000).